

## DEVELOPMENT OF A NEW CONTROLLED THERMAL EXPANSION

### SUPERALLOY WITH IMPROVED OXIDATION RESISTANCE

Edward A. Wanner and Daniel A. DeAntonio

Carpenter Technology Corporation  
P.O. Box 14662  
Reading, PA 19612-4662

#### Abstract

A new controlled thermal expansion superalloy has been developed to address deficiencies of the currently-available, conventional controlled expansion superalloys. Carpenter Thermo-Span™ alloy represents the end result of a "modular" alloy development effort, wherein a Ni-Co-Fe-Cr austenitic matrix, optimized for controlled thermal expansivity was combined with a Cb-Ti-Al gamma-prime strengthening system. Although this alloy contains (nominally) 5 w/o Cr, its coefficient of thermal expansion at 427°C is within 25% of the conventional controlled expansion superalloys. This Cr addition provides Thermo-Span alloy with sufficient general oxidation resistance to permit use of the alloy at temperatures up to 650°C without protective coatings. In this paper, the development and physical metallurgy of Thermo-Span alloy are reviewed. In addition, the physical and mechanical properties of the new alloy are characterized and compared with those of the conventional controlled expansion superalloys.

Superalloys 1992

Edited by S.D. Antolovich, R.W. Stusrud, R.A. MacKay,  
D.L. Anton, T. Khan, R.D. Kissinger, D.L. Klarstrom  
The Minerals, Metals & Materials Society, 1992

## INTRODUCTION

The conventional controlled thermal expansion superalloys may be characterized as gamma-prime-strengthened, Ni-Fe-Co-base alloys exhibiting ferro-magnetic behavior and a relatively low coefficient of thermal expansion from room temperature to approximately 430°C. These alloys are capable of sustaining mechanical properties comparable to conventional wrought superalloys at temperatures approaching 650°C while exhibiting thermal expansion coefficients as much as 50% lower than the conventional austenitic superalloys. These unique characteristics have fostered usage of controlled thermal expansion superalloys in aircraft gas turbine engines in applications where small, positive clearances between rotating and static components are required over a wide range of operating conditions.

The current family of controlled expansion superalloys has evolved over the past 20 years, with each new alloy developed to address specific shortcomings of the preceding alloy. These alloys have shared a common Ni-Fe-Co matrix, each containing 13-16% Co, approximately 38% Ni, and 40-43% Fe. A more complete documentation of their nominal compositions is provided in Table I. The history and physical metallurgy of these alloys has been addressed in several earlier publications.<sup>(1,2)</sup>

**Table I - Earlier Low Expansion Superalloys**

Element	Pyromet <sup>®</sup> CTX-1 INCOLOY* 903	Pyromet CTX-3 INCOLOY 907	Pyromet CTX-909 INCOLOY 909
Si	0.20	0.20	0.4
Ni	37.7	38.0	38.0
Co	16.0	13.0	13.0
Cb	3.00	4.8	4.8
Ti	1.75	1.5	1.5
Al	1.00	0.10	0.05
B	0.007	0.005	0.005
Fe	Balance		

Compositions Shown in Weight Percent

\* - Registered trademark of INCO family of companies

Through the use of conventional controlled thermal expansion superalloys, aircraft gas turbine engine manufacturers have realized benefits in operating efficiency. However, since these alloys do not contain chromium, they suffer from an inherent lack of oxidation resistance. This deficiency becomes critical at temperatures of 540°C and above, where protective coatings are necessary to prevent excessive oxidation of parts. Accentuating this

problem is the susceptibility of several of the conventional alloys to stress-accelerated grain boundary oxidation (SAGBO), a phenomenon wherein rapid oxidation of the grain boundaries leads to stress rupture notch sensitivity. In addition, the stability of the  $\gamma'$  strengthening precipitate of the conventional controlled thermal expansion superalloys is insufficient for sustained usage at temperatures of 650°C or above.

With the expectation of increased operating temperatures in the components where controlled thermal expansion superalloys are used, it became clear that an oxidation resistant controlled expansion superalloy was needed to eliminate the need for costly coating operations. It was also clear that this alloy should provide enhanced thermal stability, permitting operating temperatures above 650°C.

Development goals were established to guide and monitor the alloy design effort. A Ni-Co-Fe-base alloy system was selected to ensure compatibility with existing wrought superalloys, since welded assemblies are often heat treated as units. Since operating temperatures for components manufactured from this new alloy were expected to be relatively low (in the 540-700°C regime), chromium was selected as the alloy addition to enhance resistance to environmental degradation. Precipitation strengthening systems likely to cause formation of either  $\gamma'$  or  $\gamma''$  were evaluated. The hardening element additions were selected to provide mechanical properties equivalent to the existing controlled thermal expansion superalloys. The adverse

effects of chromium on the thermal expansion characteristics of this type of alloy were well known.<sup>(3)</sup> Therefore, a further design goal of this program was to adjust the matrix composition to accept a sizeable Cr addition without exceeding the thermal expansion coefficient of Pyromet® CTX-909 alloy by more than 25% at 427°C. It was also desired to minimize the process sensitivity of the new alloy to permit greater flexibility in both hot working and heat treating processes than are viable with alloy 909.

### Alloy Development

In assessing the thermal expansion characteristics of a precipitation strengthened alloy in the fully heat treated condition, the material may be viewed as a metal matrix composite. The strengthening constituent; in this case, the  $\gamma'$  or  $\gamma''$  precipitate; is of relatively fixed composition, and therefore possesses fixed expansion characteristics. The matrix constituent, a Ni-Co-Fe austenite, is not of fixed composition and may be tailored to provide minimum expansivity within the temperature range of interest. Assuming that the interactive effects between the particles and the matrix are small and unfavorable (i.e. the strain fields associated with the  $\gamma'$  or  $\gamma''$  particles increase expansivity), it becomes clear that the greatest gains can be realized through optimization of the matrix composition. Under these assumptions, a "modular" approach was employed to explore this new alloy system.

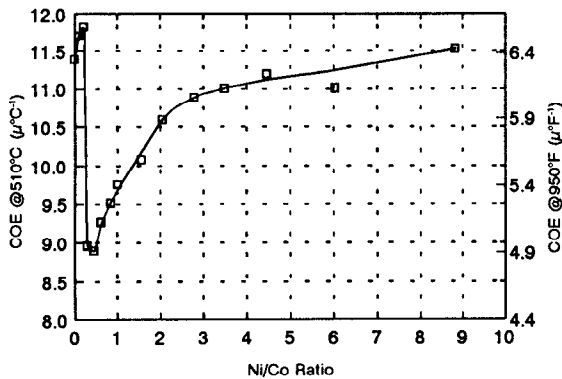


FIGURE 1 EFFECT OF NI/CO ON THE EXPANSION COEFFICIENT AT A CONSTANT NI+CO OF 50 W/O AND 6.5 W/O CR.

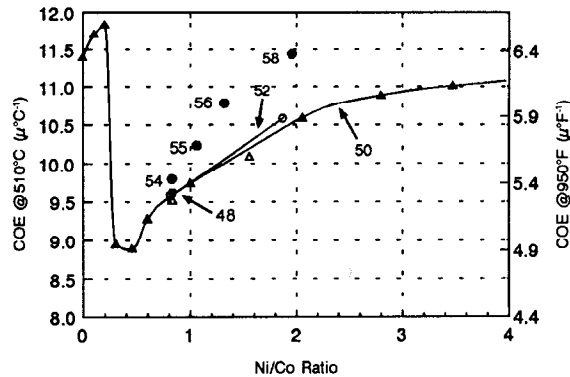


FIGURE 2 EFFECT OF NI/CO AND TOTAL NI+CO ON THE EXPANSION COEFFICIENT AT A CONSTANT 6.5 W/O CR.

Small-scale laboratory melts (70g) containing only the matrix elements Ni, Co, Fe, and Cr were processed and subsequently expansion tested to define the expansion characteristics of the austenitic matrix. The effect of varying proportions of Ni to Co at a constant Ni+Co content of 50 wt.% are shown in Figure 1. Matrix compositions having Ni/Co ratios less than 2 were explored more fully to characterize the effects of adjusted total Ni+Co content. As is evident in Figure 2, expansivity of the austenitic matrix in the temperature range of interest is minimized at a Ni/Co ratio of approximately 0.4 and a total Ni+Co content of 50 wt.%.

Investigations of the effects of various Cr contents on several of the austenitic matrix compositions evaluated yielded the expected results. Increased Cr content led to increased expansivity at all temperatures, and in addition, resulted in decreased inflection temperature (the temperature at which the ferromagnetic to paramagnetic transition occurs).

The other component of the alloy system, the strengthening precipitate, was also evaluated using laboratory VIM heats (7.7-kg). Various combinations of the

$\gamma'$ - and  $\gamma''$ -forming elements Ti, Al, and Cb were examined in proportions patterned after existing superalloys using an "interim" Ni-Co-Fe-Cr austenitic matrix as a "host." Alloy compositions were calculated based on assumptions of the most likely precipitate to form ( $\gamma'$  or  $\gamma''$ ) and the likely extent of completion of the aging reaction to be attained during heat treatment. Using published data on elemental partitioning in  $\gamma'$ <sup>(4)</sup>, the contents of Ni, Co, Cr, and Fe necessary to accommodate the 5.0 at % hardener element (Ti+Al+Cb) additions were calculated. Based upon the results of screening tests for strength and oxidation resistance capabilities, a Cb-rich system with Cb, Ti and Al proportioned after alloy 718 was selected.

### Alloy Optimization

The optimum matrix composition and hardener system determined in the earlier studies were combined using the previously discussed partitioning coefficients and precipitation completeness assumptions to arrive at the base composition listed in Table II. Small-scale laboratory heats (7.7-kg) were melted to evaluate the properties of this base composition as well as variant compositions characterizing

**Table II - Alloy Optimization Matrix**

	Base Composition	Experimental Range
Ni	26	24 - 27
Co	27	26 - 29
Cr	5.5	3.5 - 7.2
Si	0.35	0.1 - 0.5
Cb	4.8	3.8 - 5.3
Ti	0.85	0.6 - 1.0
Al	0.45	0.3 - 0.5
B	0.004	---
Fe	Balance	---

**Table III - Nominal Composition of Carpenter THERMO-SPAN Alloy**

Ni	-	24.5
Co	-	29.0
Cr	-	5.5
Si	-	0.35
Cb	-	4.8
Ti	-	0.85
Al	-	0.45
B	-	0.004
Fe	-	Balance

the effects of Cr, Si, and the hardener elements (Ti+Cb+Al) over the ranges shown in Table II. These heats were vacuum induction melted and forged to bar stock for preliminary testing. Based on the results of these tests, the final Thermo-Span™ alloy composition (Table III) was developed.

### Physical Metallurgy

The microstructure of Thermo-Span alloy, like that of 909 alloy, contains a uniform distribution of coarse, globular precipitates in the as-hot-worked condition as shown in Figure 3. Analysis of this globular precipitate (Table IV) revealed its composition to differ from that of the similar precipitate in alloy 909. However, the differences are thought to be due to differences in the bulk alloy composition, eg. substitution of Co for Ni in the Thermo-Span alloy precipitate as compared with the alloy 909 precipitate. The presence of this type of phase has been shown to contribute substantially to the stress rupture ductility of several Cr-free controlled expansion superalloys.<sup>(5,6)</sup> Additionally, since the solvus temperature of the globular precipitate in Thermo-Span alloy is quite high (>1093°C), some measure of grain size control is achieved through the presence of this phase at the standard solution treating temperature.

The strengthening precipitate in Thermo-Span alloy has been identified as  $\gamma'$  via electron diffraction. The  $[001]_{fcc}$  zone axis diffraction pattern of Figure 4 shows

**Table IV** - Composition Comparison of Globular Phases in THERMO-SPAN Alloy and Pyromet CTX-909 Alloy

Element	CTX-909	THERMO-SPAN
Fe	18	20
Ni	38	17
Co	14	28
Cb	18	18
Ti	3	1.3
Si	5	12
Cr	0	2

All Analyses in Atomic Percent

the absence of the characteristic  $\{1\bar{1}0\}$  superlattice reflections indicative of  $\gamma^{n(7)}$ , together with the presence of the  $\{100\}$  superlattice ( $\gamma'$ ) reflections. Figure 5 shows the uniform distribution of fine (13-17 nm) cuboidal  $\gamma'$  resulting from the standard heat treatment (1093°C/1 hr./AC + 718°C/8 hr./FC @ 56°C/hr. to 621°C/8 hr./AC).

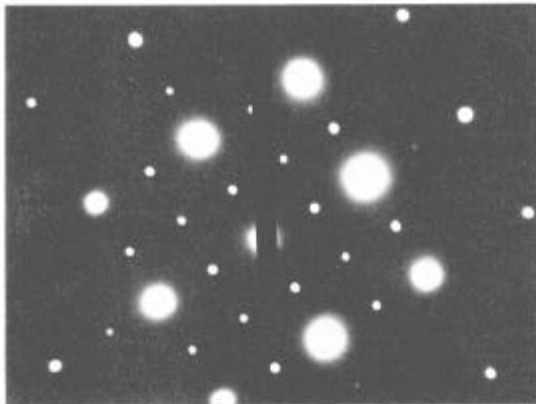


**FIGURE 4** ELECTRON DIFFRACTION PATTERN OF  $[001]_{FCC}$  ZONE AXIS.

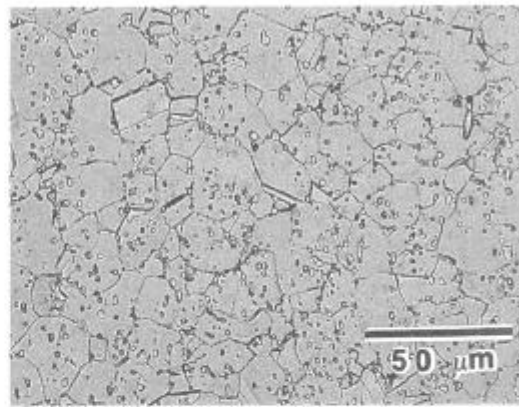


**FIGURE 3** MICROSTRUCTURE OF THERMO-SPAN ALLOY IN THE FULLY TREATED CONDITION SHOWING UNIFORM GLOBULAR PHASE DISTRIBUTION.

ETCHANT: WATERLESS KALLING'S

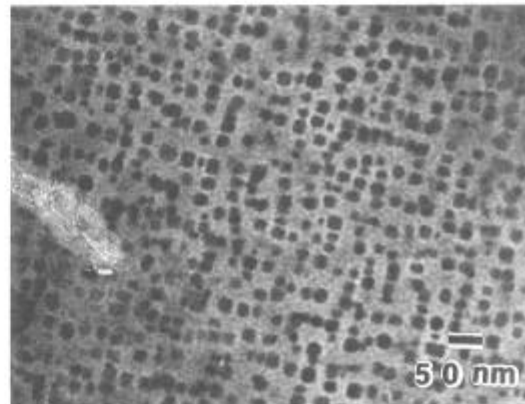


**FIGURE 5** TEM MICROGRAPH OF THIN FOIL SHOWING UNIFORM  $\gamma'$  DISTRIBUTION.

#### Characterization of Thermo-Span Alloy

A production-size heat (4500 kg) was vacuum-induction melted and vacuum-arc remelted, followed by rotary forging to 203 mm diameter billet. To obtain specimens for mechanical property characterization, "pilot bars" were processed by press forging small transverse billet segments to 38.1 x 19.1 mm flats. Test specimen coupons were solution treated 1093°C/1 hr./Air Cool followed by double aging at 718°C/8 hr./furnace cool at 56°C/hr. to 621°C/8 hr./Air Cool. The foregoing heat treatment is the standard heat treatment for Thermo-Span alloy.

#### Oxidation Resistance

The susceptibility of Thermo-Span alloy to oxidation in static, high temperature air was assessed using a cyclic exposure test. Machined right cylindrical specimens (12.7 mm dia. x 12.7 mm long) contained in porcelain glazed crucibles were exposed in an electrically-heated laboratory furnace at 677°C using a 20 hr. on heat, 4 hour cooling cycle for 52 cycles (1040 total hrs. on heat). Lids were placed on the crucibles during cooling to contain any spalling oxide. Identical specimens machined from alloy 718 and from alloy 909 were tested simultaneously for reference.

The oxidation weight-gain data of Figure 6 show Thermo-Span alloy to provide an order of magnitude improvement in oxidation resistance over alloy 909. In addition, the cyclic oxidation rate of Thermo-Span alloy is markedly lower than alloy 909, and approaches that of alloy 718.

### Thermal Expansion

A primary goal of the alloy development effort was to provide enhanced oxidation resistance coupled with minimally increased thermal expansivity in comparison with the conventional controlled expansion superalloys. The test data of Table V and Figure 7 show that the development goal of a maximum 25% increase in thermal expansion coefficient at 427°C over the conventional alloys was achieved. In addition, it is important to note that, with the exception of the lower inflection temperature of Thermo-Span alloy, the thermal dilation profiles ( $\Delta l/l$  curves) of the two alloys shown in Figure 7 are similar. This feature allows the use of Thermo-Span alloy as a direct replacement for alloy 909 at usage temperatures below ~320°C. In addition, the fact that the  $\Delta l/l$  curves for both alloys are parallel above their inflection temperatures indicates that these alloys will behave similarly in applications where temperatures cycle between ~430 and 650°C (provided the differences in behavior during heat-up to 430°C are taken into account).

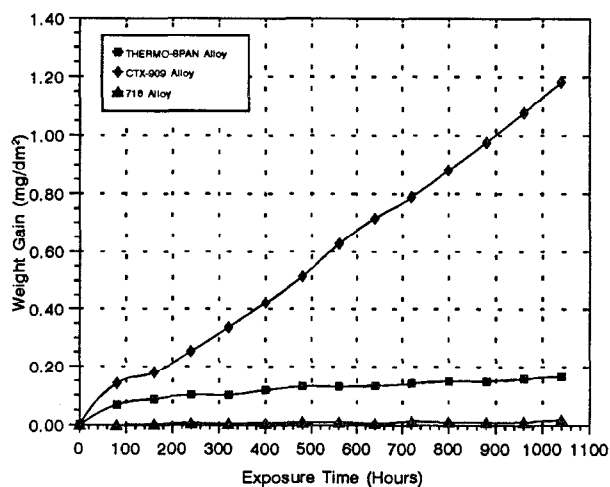


Figure 6 COMPARATIVE CYCLIC OXIDATION WEIGHT GAIN. CYCLED 20 HR. AT 677°C/ 4 HR. AT ROOM TEMPERATURE.

Table V - Thermal Expansion Coefficients for THERMO-SPAN Alloy and Alloy 909 at Various Temperatures

Temp. (°C)	THERMO-SPAN Alloy COE ( $\mu\text{C}^{-1}$ )	Alloy 909 COE ( $\mu\text{C}^{-1}$ )	Temp. (°F)	THERMO-SPAN Alloy COE ( $\mu\text{F}^{-1}$ )	Alloy 909 COE ( $\mu\text{F}^{-1}$ )
-184	7.29	---	-300	4.05	---
-129	7.70	---	-200	4.28	---
-73	7.94	---	-100	4.41	---
-18	8.10	---	0	4.50	---
93	8.06	8.1	200	4.48	4.5
204	7.72	7.7	400	4.29	4.3
316	8.21	7.8	600	4.56	4.2
427	9.76	7.7	800	5.42	4.3
538	11.05	9.0	1000	6.14	5.0
649	12.15	10.4	1200	6.75	5.8
Inflection Temp.	321°C	427°C	610°F	800°F	

### Tensile Properties

The room and elevated temperature tensile data of Table VI and Figure 8 show that Thermo-Span alloy provides useful strength to approximately 677°C. In comparison with conventional controlled expansion superalloys, Thermo-span alloy provides comparable tensile strength together with the ability to use significantly higher solution treating temperatures. In the case of alloy 909, high temperature "overaging" heat treatments must be used to restore stress rupture notch ductility

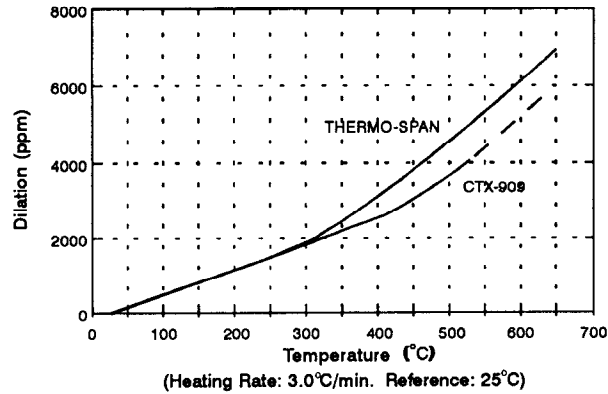


Figure 7 COMPARATIVE  $\Delta l/l$  curves for Thermo-Span alloy and alloy 909.

when solution treating temperatures of 1024°C or higher are used. Thermo-Span alloy also provides a significant improvement in elastic modulus when compared to the conventional controlled expansion superalloys. This property is of concern for components that are designed for applications limited by buckling.

Table VI - Tensile Properties of THERMO-SPAN Alloy  
(Production Heats)

Test Temperature	0.2% Y.S. (MPa) (ksi)		U.T.S. (MPa) (ksi)		Elong. (%)	R.A. (%)
RT	952	138	1310	190	15	35
	952	138	1303	189	15	34
	931	135	1303	189	16	36
677°C (1250°F)	766	111	979	142	22	40
	752	109	959	139	21	42
	759	110	959	139	19	27

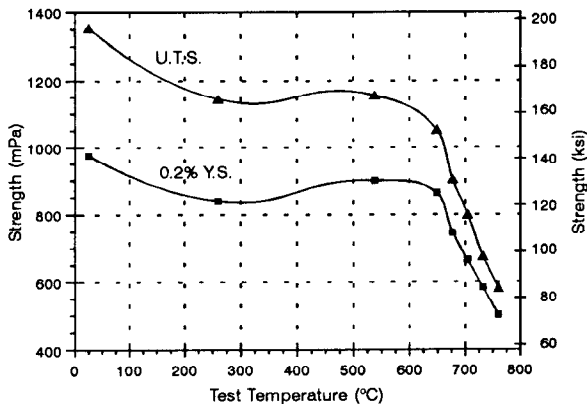


Figure 8 EFFECT OF TEST TEMPERATURE ON THE TENSILE STRENGTH OF THERMO-SPAN ALLOY.

### Stress Rupture and Creep Properties

The typical 538°C, 649°C, and 677°C stress rupture properties of Thermo-Span alloy are shown in Table VII. The test conditions employed in this series of tests are typical of those normally used in testing conventional controlled expansion superalloys, with the exception of the 677°C/510 MPa test which is specific to Thermo-Span alloy. It is worth noting that no notch breaks were encountered in the combination bar tests conducted at 649 and 677°C, indicating that Thermo-Span alloy is not sensitive to SAGBO under

these conditions.

The nominal creep characteristics of Thermo-Span alloy at 649 and 704°C are presented in Figure 9. The stress necessary to generate 1.0% creep strain in 100 hr. at 649°C for Thermo-Span alloy is approximately 655 MPa, which is nearly equivalent to alloy 718 (689 MPa required to generate 1.0% creep strain in 100 hr. at 649°C<sup>(8)</sup>). At 704°C, the same creep strain was generated with a stress level of 345 MPa for

**Table VII - Stress Rupture Data for THERMO-SPAN Alloy**  
1093°C Solution Treated + 718/621°C Age

Test Temperature	Stress (MPa)	Stress (ksi)	Specimen Type	Rupture Life (hr.)	Elong. (%)
538 °C (1000°F)	828	120	Notch ( $K_t = 2$ )	511.9	--
				980.4	--
649 °C (1200°F)	510	74	Combo ( $K_t = 3.8$ )	800.1	17.8
				1047.9	29.3
677 °C (1250°F)	510	74*	Combo ( $K_t = 3.8$ )	106.0	21.3
				94.4	18.7
				93.2	16.8

\* - Specimens unloaded 34.5 MPa (5 ksi) every 8 to 16 hours after initial 48 hours. The load at failure for the three specimens was 614 MPa (89 ksi), 648 MPa (94 ksi) and 648 MPa (94 ksi) respectively.

Thermo-Span alloy, while a stress of 496 MPa was required for alloy 718<sup>(8)</sup>.

### Fatigue Properties

Room temperature high cycle fatigue testing was conducted using the R. R. Moore rotating beam fatigue test. The resultant fatigue curve (Figure 10) shows that the endurance limit of Thermo-Span alloy is approximately 550 MPa, which compares favorably with alloy 909 under identical test conditions.<sup>(9)</sup>

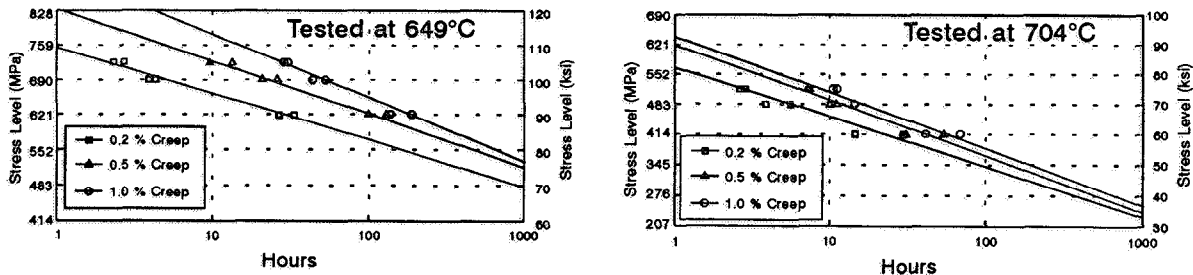


**Figure 9 CREEP CURVES FOR THERMO-SPAN ALLOY.**

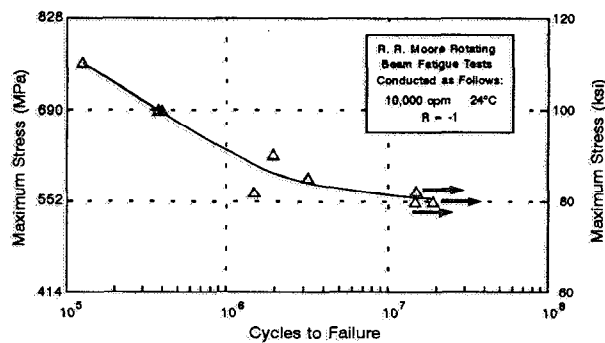


**Figure 10 HIGH CYCLE FATIGUE PROPERTIES OF THERMO-SPAN ALLOY.**

### Thermal Stability

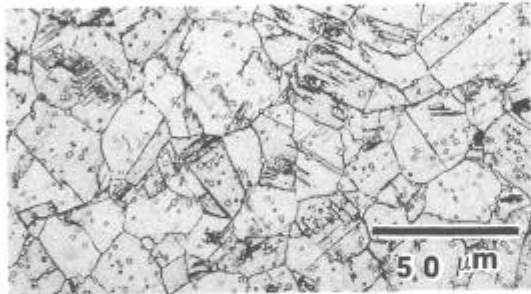
The stability of the  $\gamma'$  aging precipitate in Thermo-Span alloy after extended exposures at 677°C was measured using post-creep tensile testing. Duplicate machined specimens were exposed at 677°C in creep stands with applied stresses sufficient to generate 0.3% creep strain in approximately 300h. Creep exposures were discontinued after 0.3% creep strain was attained. Simultaneously, a set of duplicate specimens was exposed at 677°C for 300 hr. in a heat treating furnace with no applied stress. Each of these exposed specimens was subsequently tested in tension at room temperature to determine the effect of 677°C thermal exposure on the  $\gamma'$  strengthening phase. As an additional evaluation, one specimen from each set was tested with the oxide scale formed during the 677°C exposure intact, while the other was turned to remove all oxide scale. The results of the post-creep and post-exposure tensile tests are presented in Table VIII and demonstrate good bulk stability and surface integrity. The primary microstructural change accompanying the 677°C creep exposure was formation of a fine dark-etching precipitate on grain boundaries and slip lines (Figure 11a). The 677°C static exposure specimen (no applied stress) showed some enhanced grain boundary precipitation, but lacked intragranular precipitation (Figure 11b). No needle-like overaging precipitates (eg.  $\delta$ ,  $\eta$ , or  $\epsilon$ ) were observed in the specimens.



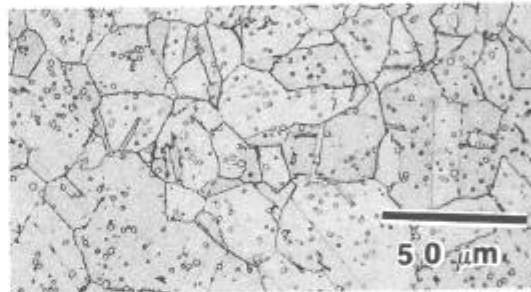
**Table VIII - Room Temperature Tensile Properties of THERMO-SPAN Alloy Specimens\* After 300 hr. Exposure at 677°C (with and without loading)**

Loading**	Surface Removal	0.2% Y.S. (MPa) (ksi)		U.T.S. (MPa) (ksi)		Elong. (%)	R.A. (%)
No	Yes	855	123.9	1185	171.8	15.9	28.9
Yes	Yes	828	120.0	1169	169.5	16.0	34.7
No	No	851	123.4	1182	171.4	17.0	34.8
Yes	No	819	118.8	1140	165.3	20.0	38.6
Unexposed H/N 88475***		876	127.0	1228	178.0	18.0	32.0

\* - Specimen Solution Treated at 1093°C/1hr./AC + Aged 718°C/8hr./FC @ 48°C/hr. to 621°C/8hr./FC  
 \*\* - Specimens loaded to produce 0.3% creep in 300 hours  
 \*\*\* - Data obtained from production tests



a. 0.3% CREEP STRAIN



b. NO CREEP STRAIN

**Figure 11 MICROSTRUCTURE OF THERMO-SPAN ALLOY AFTER EXPOSURE AT 677°C FOR 300 HR. ETCHANT: WATERLESS KALLING'S**

### Summary

A new controlled thermal expansion superalloy has been developed which addresses several of the shortcomings of the conventional controlled expansion superalloys available today. Carpenter Thermo-Span alloy utilizes a small (5.0 w/o) Cr addition to a  $\gamma'$ -strengthened, Ni-Co-Fe austenitic matrix to provide sufficient general oxidation resistance to permit uncoated usage at temperatures up to 650°C. In addition, this alloy provides thermal expansivity levels within 25% of the Cr-free, conventional alloys to 427°C. The  $\gamma'$  precipitate of Thermo-Span alloy is thermally stable to 677°C (28°C higher than the conventional alloys), and provides comparable strengths to the conventional alloys at the lower temperatures. Thermo-Span alloy is strengthened using a conventional two-step aging cycle (718°C/621°C) making final heat treatment of welded, dual-alloy components feasible. In addition, grain size control during high-temperature manufacturing operations (eg. brazing, forging, solution treating) is provided by a stable Laves-type precipitate, allowing exposures at temperatures of 1093°C and above without unacceptable grain growth.

### Acknowledgements

The efforts of Mr. D. A. Englehart in the preparation of the graphics for this paper and Mr. J. W. Bowman for the electron microscopy are gratefully acknowledged.

## References

1. D. F. Smith and J. S. Smith, "A History of Controlled, Low Thermal Expansion Superalloys," Physical Metallurgy of Controlled Expansion Invar-Type Alloys, ed. K. C. Russell and D. F. Smith (Warrendale, PA: The Metallurgical Society, 1990), pp. 253-272.
2. E. A. Wanner, et al., "The Current Status of Controlled Thermal Expansion Superalloys," JOM, 43(3) (1991), 38-43.
3. R. M. Bozorth, Ferromagnetism, (N.Y.: Van Nostrand, 1951).
4. O. H. Kriege and J. M. Baris, "The Chemical Partitioning of Elements in Gamma Prime Separated from Precipitation-Hardened, High-Temperature Nickel-Based Alloys," Transactions of the ASM, 62 (1969), 195-200.
5. K. A. Heck, et al., "The Physical Metallurgy of a Silicon-Containing Low Expansion Superalloy," Superalloys 1988, ed. D. N. Duhl, et al., (Warrendale, PA: The Metallurgical Society, 1988), 151-160.
6. E. A. Wanner and D. A. DeAntonio, "Development of a New High Strength Controlled Thermal Expansion Superalloy," Physical Metallurgy of Controlled Expansion Invar-Type Alloys, ed. K. C. Russell and D. F. Smith, (Warrendale, PA: The Metallurgical Society, 1990), 301-313.
7. D. F. Paulonis, J. M. Oblak, and D. S. Duvall, "Precipitation in Nickel-Base Alloy 718," Transactions of the ASM, 62 (1969), 611-622.
8. Aerospace Structural Metals Handbook, (1991) Vol 4, Code 4103, page 36.
9. D. F. Smith and J. S. Smith, "A Silicon-Containing, Low-Expansion Alloy with Improved Properties", Superalloys 1984, ed. M. Gell, et al., (Warrendale, PA: The Metallurgical Society, 1984) 591-600.